Statistical Downscaling and Bias Correction of the Earth System Models (ESM) Outputs for Future Climate Projection under Solar Geoengineering: Case Study Indonesia

F. Fauzi
Dept. of Statistics, Universitas Muhammadiyah Semarang, Indonesia

*H. Kuswanto**
Dept. of Statistics, Institut Teknologi Sepuluh Nopember, Indonesia
** heri_k@statistika.its.ac.id*

R. M. Atok
Dept. of Actuarial Science, Institut Teknologi Sepuluh Nopember, Indonesia

M. Salamah
Dept. of Business Statistics, Institut Teknologi Sepuluh Nopember, Indonesia

ABSTRACT

Solar Radiation Management (SRM) is a controversial idea for minimizing global warming. Simulations have been carried out to generate the future projection of the climate condition from the Earth System Models (ESM). However, the outputs are available on low-resolution data with some degree of bias. Downscaling is a solution to obtain ESM data that resembles the local climate. This study also applied several popular bias correction methods to correct the bias of Marine-Earth Science and Technology (MIROC)-ESM historical data and further assessed the significance test for each grid through correlation map and Taylor diagram. Extreme index (e.g. the max 1-day precipitation amount (RX1Day) and the hottest day (TXx)) projected with SRM and without SRM is derived, based on the downscaled output and the best correction bias. We found an inconsistent pattern of difference Rx1Day index between with and without SRM scenarios, while the TXx index of the with SRM

ISSN 1823-5514, eISSN 2550-164X
Received for review: 2020-09-09
Accepted for publication: 2021-01-20
Published: 2021-11-15

scenario is consistently below the without SRM scenario. It indicated that SRM will effectively reduce the level of future maximum temperature.

Keywords: *Statistical Downscaling; Bias Correction; Climate Projection*

Introduction

The large-scale El-Nino-Southern Oscillation (ENSO) is one of the causes of climate change in Indonesia [1, 2]. El-Nino is strongly associated with rainfall in Indonesia, especially on the southern equatorial islands (Java, Bali, and Nusa Tenggara) during the dry season (June-August) and transition (September-November) [3]. Besides ENSO, the greenhouse effect also influences climate change in the 21st century. The earth's temperature will increase 1-3.7 ˚C depending on future greenhouse gas emissions [4]. The Intergovernmental Panel on Climate Change (IPCC) in 2018 reported that the current temperature rise was between 1.5 ˚C - 2.0 ˚C as a result of the greenhouse effect [5]. The causes of the greenhouse effect include emissions from engines emitting various gases such as HCs, CO_2. The increasing number of exhaust emissions is directly proportional to the need for increased fuel consumption. Reducing pollution will reduce the rate of climate change. Future urban, transport and environmental planning that can adapt to climate change will be a good idea for sustainable development. In this case, the engineering profession such as mechanical engineer plays a significant role in addressing climate change [6].

Based on the statistics reported by the National Disaster Management Agency (BNPB), in 2019 there were 3724 forest fires, 1529 droughts, and 1276 floods, some of which have increased from previous years. Oktaviani et al. [7] found that Indonesia will experience an increase in temperature by 0.8 ˚C in 2030, which will have an impact on changing rainfall patterns and shorter rainy seasons. Moreover, the situation will significantly impact the economic and agricultural sectors [8]. Climate change mitigation efforts in the future, regional development strategies lead to urban greening, public transportation, and environmentally friendly energy [9]. The impact of climate change will also impact some urban areas because most of Indonesia's population resides in cities [10]. Sipayung et al. [11] predict that climate change will induce drought leading to a very dry in August 2022, 2024, 2028, 2030, and 2033 on the island of Sumba. Kuswanto et al. [12] found that East Nusa Tenggara had experienced about 25 months of drought from 1999 to 2015.

The theoretical approach to controlling climate change by reflecting a small amount of sunlight entering the earth back out of space is the basic idea of Solar Radiation Management (SRM) or solar geoengineering. Reflection of sunlight into space by aerosol injection in the stratosphere is one of the efforts

to cool the earth. The impact of SRM was investigated by Kravitz et al. [13] by conducting experiments on 4 The Geoengineering Model Intercomparison Project (GeoMIP) scenarios namely G1, G2, G3, and G4. SRM does not give impact only on climate and weather, but also on socioeconomic, health, and other related aspects. The impact of SRM on agriculture is estimated to be quite complex. Most crops benefited from cooling under the SRM scenario, but not rice and peanuts in ASIA [14]. During the last 15 years (2055 - 2069) the injection period of GeoMIP G4 was able to increase 5.3 ± 5.7% of rice production in China. [15]. Parkes et al. [16] found contradictory effects of geoengineering climate schemes. In Northeast China and West Africa, where in Northeast China there was an increase in crop failure while in West Africa there was a reduced risk of crop failure due to the doubling of carbon dioxide in the atmosphere. The other researches on the impacts of SRM on the agricultural sector have been investigated by [14, 15]. Indonesia has a tropical climate and most people work on farming activities that are highly dependent on weather and climate conditions. Therefore, it is necessary to study the effects of geoengineering in Indonesia. The SRM strategy can also impact human health from surface aerosol deposition [19]. Besides having an impact on the agricultural and health sectors, SRM also has an impact on the social, economic and political fields as previously investigated by [20]–[22]. Ji et al. [23], Kravitz et al. [24], and Irvine et al. [25] investigated other effects of geoengineering on climate and weather.

Most of the studies show the significant effect of SRM to reduce global temperature, however, these studies were mostly conducted in developed countries. It is very important to study the impact of SRM in Indonesia. In addition to developing countries, Indonesia's geographical location is on the equator, which has a tropical climate and is vulnerable to the effects of climate change. A study has been conducted in South Africa found a significant decrease in mean temperature extremes in South Africa after aerosol injection into the stratosphere [26]. Another study by Karami et al. [27] has been focused on the scenario of Stratospheric Aerosol Geoengineering (SAG) in storm pathways in MENA region. Da-Allada et al. [28] compared SAG with RCP8.5 in the regions of the North Sahel, Southern Sahel, and West Africa and found that during the monsoon period the rainfall under the RCP8.5 scenario increased by 44.76%, 19.74%, and 5.14%, while the climate under the SAG scenario the rainfall decreased by 4.06% (0.19 ± 0.22 mm) and 10.87% (0.72 ± 0.27) mm) in the Southern Sahel and West Africa. Based on the three studies above, it produces different conclusions in each region.

Conducting a local impact study on SRM requires a high-resolution dataset to obtain information that represents the real condition of the targeted area. Unfortunately, the Earth System Models (ESM) dataset generated from the climate scenarios is available on low-resolution data covering a large spatial scale. Therefore, downscaling and bias correction need to be carried

out. Converting large-scale grids of General Circulation Models (GCM) data into small-scale grids is a function of the downscaling technique [29]. The downscaling method provides a computationally efficient and effective way to generate plausible hydro-climatology from large ensembles [30]. In recent years, methods that combine statistical downscaling have been developed with bias correction, to minimize the bias of downscaling results which are more representative of the local climate. Among the popular downscaled and bias correction methods are Quantile Delta Mapping (QDM), Bias Correction/ Constructed Analogues with Quantile Mapping (BCCAQ) and Inter-Sectoral Impact Model Intercomparison Project (ISI-MIP).

Bias-Correction and Spatial Disaggregation (BCSD) can produce better results on the Parallel Climate Model (PCM) data compared to linear interpolation and spatial disaggregation methods [31]. Another bias correction method introduced by Piani et al. [32] is quantile mapping. The method that is capable of synthesizing the share of global warming levels in the agriculture, water, biome, health, and infrastructure sectors is the ISI-MIP [33]. The ISI-MIP method has been developed to maintain signals of changing climate trends. Quantile mapping can eliminate bias, but quantile mapping can destroy the trend of future model projections [34]. BCCAQ downscaling method can produce more accurate results by improving the weaknesses of its predecessor method. BCCAQ can reduce the global scale to the local scale for the case of rainfall and temperature well [35]. Several previous studies have investigated the performance of e the QDM, BCCAQ, and ISI-MIP methods [36]–[43]. This paper investigates the performance of the three different methods in producing the best-downscaled climate projections and bias corrections for historical periods. Furthermore, the best method is applied to derive the two extreme indices, resulting from the MIROC-ESM scenario under SRM and RCP4.5.

Data and Methodology

In this research, ESM output will be downscaled using the ERA-Interim European Centre for Medium-Range Weather Forecasts (ECMWF) data as the proxy of the observation dataset. The downscaling results in the ESM output will then be bias-corrected to obtain results that can explain the local climate. This paper examines three bias correction methods i.e. QDM, BCCAQ, and ISI-MIP. ESM output in this study consists of three scenarios, namely historical, Representative Concentration Pathway (RCP) 4.5, and G4 GeoMIP experiment. RCP4.5 is a long-term global greenhouse gas emission scenario that by 2100 maintains radiation emissions of around 4.5 Wm^{-2} (about 650 ppm CO_2 equivalent) [44]. Continuous injection of 5 Tg SO_2 into the

stratosphere is a GeoMIP experiment in the G4 scenario introduced by Kravitz et al. [13]. Following are the G4 and RCP4.5 scenarios.

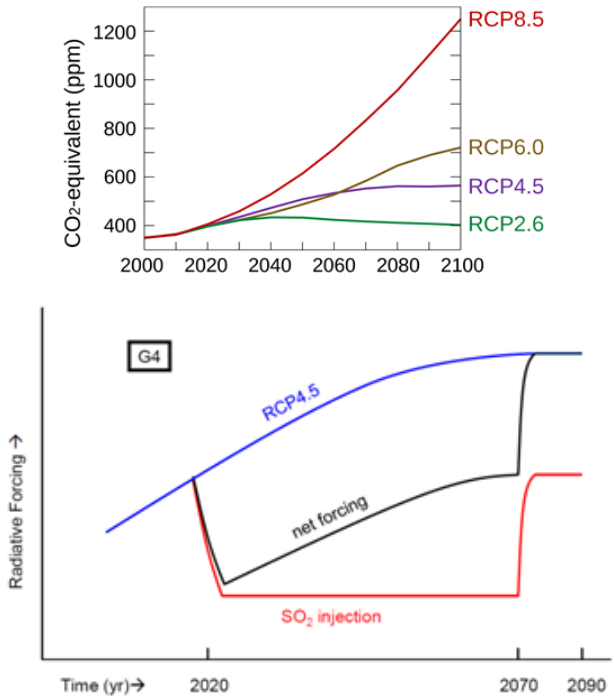

Figure 1: G4 and RCP4.5 scenarios (Kravitz et al [10]).

There are two data sources used in this study. The first data source comes from the Coupled Model Intercomparison Project Phase 5 (CMIP5) and the second data source comes from the European Centre for Medium-Range Weather Forecasts (ECMWF). The details of the data are as follows

Table 1: Summary of datasets used in the analysis

Data	Scenario	Resolution	Scale
Marine-Earth Science and Technology (MIROC) Earth System Model (MIROC-ESM)	Historical	2.8° × 2.8°	Daily
	G4	2.8° × 2.8°	Daily
	RCP4.5	2.8° × 2.8°	Daily
ERA-Interim	-	0.25° × 0.25°	Daily

The QDM method is a bias correction method that can maintain relative changes in the future [34]. The QDM method for rainfall is as follows:

$$\hat{x}_{m,p}(t) = F_{o,h}^{-1}\left\{F_{m,p}^{(t)}\left[x_{m,p}(t)\right]\right\}\left[\frac{x_{m,p}(t)}{F_{m,h}^{-1}\left\{F_{m,p}^{(t)}\left[x_{m,p}(t)\right]\right\}}\right] \quad (1)$$

The bias correction for the temperature variable is used as an additive process with the following equation:

$$\hat{x}_{m,p}(t) = x_{m,p}(t) + F_{o,h}^{-1}\left\{F_{m,p}^{(t)}\left[x_{m,p}(t)\right]\right\} - F_{m,h}^{-1}\left\{F_{m,p}^{(t)}\left[x_{m,p}(t)\right]\right\} \quad (2)$$

where $(F_{m,h})$ is the cumulative distribution (CDF) of ESM output in the historical period, $(F_{0,h})$ is the CDF of observation in the historical period, and $(F_{m,p})$ is the CDF of the future ESM output 'Projection'. Whereas $x_{o,h}$ represents the rainfall or temperature data from observations in the historical period, ESM outputs in historical and future periods are $x_{m,h}$ and $x_{m,p}$. The results of future bias correction on rainfall or temperature data are denoted by $\hat{x}_{m,p}$.

The combination of the output climate analogues introduced by Hidalgo et al. [45] and quantile mapping at fine-scale resolution by Piani et al. [32] resulted in a BCCAQ downscaling hybrid method. Bias correction for Quantile Delta Mapping (QDM) is carried out separately for each algorithm (Constructed Analogs (CA) algorithm and Climate Imprint (CI) algorithm), which is the first stage of the BCCAQ method [34]. Combining CI and CA outputs by taking daily QDM results at each local scale grid point and rearranging them in certain months according to daily CA rankings using empirical copula is the process of the BCCAQ method [35].

The correction of bias using the ISI-MIP method consists of two stages, namely long-term monthly average correction and daily variability adjustment [33]. Thus, X_{ijk}^{data} represents data for the *i*-th day, *j*-month and *k*-year, on a particular grid cell of the simulation time series (ESM data) or observation, where T is the daily average temperature data and P is the data for rainfall. A nonlinear (exponential) approach was chosen for the rainfall case, so the correction formula in the rainfall data is as follows:

$$P_{ijk}^{adj} = \left[a + b\left(P_{ijk}^{ESM} - P_{mean}^{ESM}\right)\right]\left[1 - \exp\left\{\frac{-\left(P_{ijk}^{ESM} - P_{mean}^{ESM}\right)}{c}\right\}\right] \quad (3)$$

The linear portion of the function above is represented by the offset *a* and the slope of *b*, while *c* is the decay constant for the exponential part which must be adjusted. While correcting the bias in temperature variables apply the linear function as follows:

$$\hat{T}_{ijk}^{ESM} = \delta_j + b\Delta T_{ijk}^{ESM} + \hat{\bar{T}}_{jk}^{ESM} \tag{4}$$

Where δ_j is the long-term mean temperature in the j-th month, $\hat{\bar{T}}_{jk}^{ESM}$ is the average corrected monthly temperature, ΔT_{ijk}^{ESM} is the residual ESM output and *b* is the slope.

Evaluation of our correction bias capabilities uses a Taylor diagram. Taylor diagram reflects three statistical measures namely root mean square error, correlation, and standard deviation. The method that has the best ability is the method that has the lowest Root Mean Square Error (RMSE) value and standard deviation, the biggest correlation, and approaches the observation point [46]. Furthermore, the best method is used to calculate the two extreme indices. The two indices are the hottest day (TXx) and the max 1-day precipitation amount (Rx1Day). TXx is the highest daily maximum temperature of the month [47]. Rx1Day is the max daily precipitation of the month[47].

Results and Discussion

This section will present a MIROC-ESM difference map before and after downscaling and bias correction using the three methods (QDM, BCCAQ, and ISI-MIP). Correlation maps, significance tests on each grid, and Taylor diagrams were being to evaluate the skills of the bias correction method. The best bias correction method applied for climate projection in scenarios with (G4 scenario) and without SRM (RCP4.5 scenario).

Downscaling and bias correction of Rainfall and maximum temperature data

Figure 2 presents the raw dataset (before downscaling) and after downscaling of MIROC-ESM output for rainfall and maximum temperature. Moreover, the maps of observation data i.e. ERA-Interim dataset are given as well. Figure 2 is the result of the BCCAQ bias correction method.

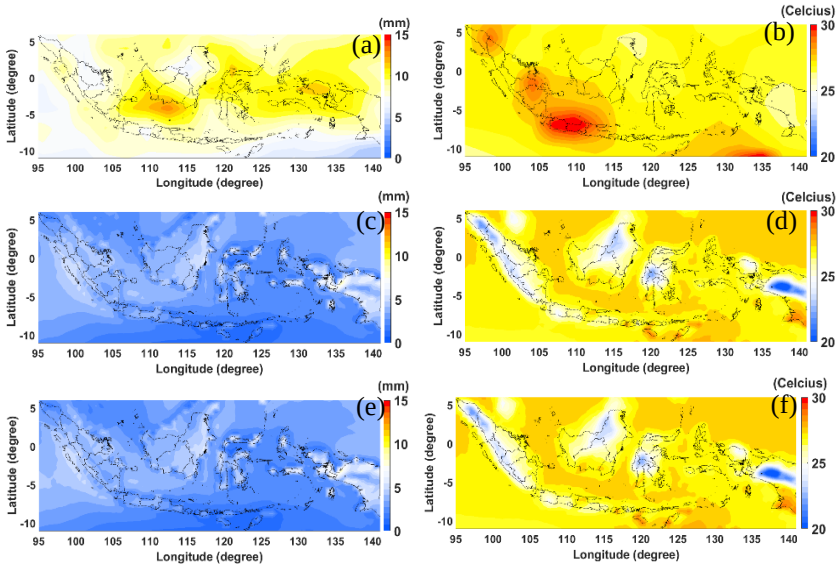

Figure 2: MIROC-ESM; (a) rainfall before downscale and bias correction, (b) maximum temperature before downscale and bias correction, (c) rainfall after downscale and bias correction, (d) maximum temperature after downscale and bias correction, (e) rainfall ERA-Interim ECMWF, and (f) maximum temperature ERA-Interim ECMWF.

The raw data has a higher rainfall intensity and maximum temperature than the ECMWF ERA-Interim (see Figure 2). After downscaling and bias correction on raw data, see Figure 2 (b) and (d), the rainfall and maximum temperature shifted the pattern following the ERA-Interim data, this shows that downscaling and bias correction can remove the bias well so that it can represent the local climate better. The highest rainfall is observed over Kalimantan, parts of Sulawesi and Papua. The lowest maximum temperature is found along the island of Sumatra and parts of Papua.

Skill Evaluation

Before choosing the downscale method and the best bias correction for climate projections, the correlations between downscaled and observation datasets will be displayed. Correlations are calculated to find out whether the results of downscale and ESM output have similar patterns with local climate (ERA-Interim ECMWF). The correlation maps are depicted in Figure 3.

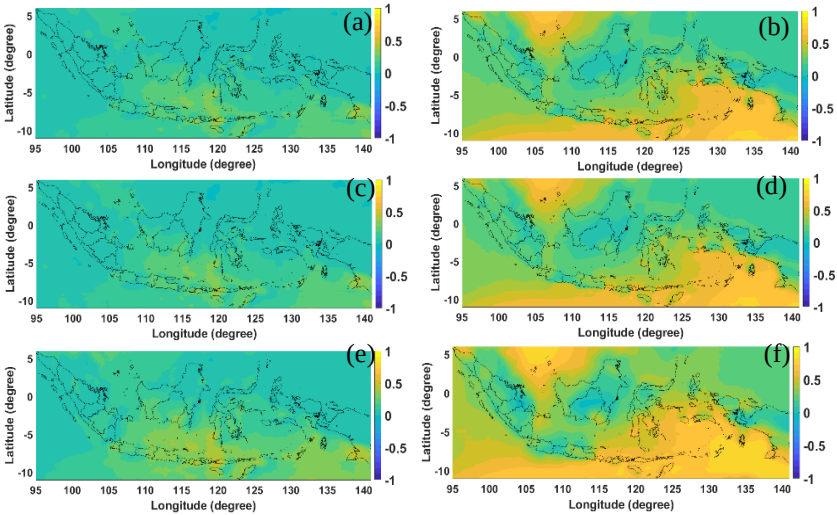

Figure 3: Correlation map of the MIROC-ESM model; (a) rainfall of the BCCAQ method, (b) temperature maximum of the BCCAQ method, (c) rainfall of the QDM method, (d) maximum temperature of the QDM method, (e) rainfall of the ISI-MIP method, and (f) maximum temperature method ISI-MIP.

The climate zone in Indonesia is divided into 3 regions based on rainfall pattern characteristics. Region 1 is a monsoon type region where the region in the region has a clear period between the dry season and rainy season, the type of rainfall in region 1 is unimodal. Region 2 is a local type region (anti-monsoon) which is the opposite of Region 1. Region 3 is an equatorial type region where the region has a bimodial rain distribution (two maximum peak rainy seasons) almost all of the year included in the rainy season criteria.

The highest value of the correlation coefficient is observed in the southern part of Indonesia, which belongs to Region 1, with coefficients ranging from 0.4 to 0.5. Region 3 is the region with the lowest correlation coefficient. The ISI-MIP method's correlation map is slightly better than the QDM and BCCAQ methods, although the difference is not significant. Furthermore, we will test the significance of correlation values along with the grids. There are 12834 points (grid) where the correlation significance will be tested. A summary of the results of the correlation significance test can be seen in Table 2. The suitability of the pattern between the output bias correction of the ESM and the reanalysis data (ERA-Interim ECMWF) can be seen from the significance of the correlation. Based on Figure 3, it can be seen that the size

of the correlation coefficient tends to group according to region, then the correlation significance test by region.

Table 2: Test the significance of the grid.

Variable	Region	Methods	Value of t table	Significant number of points (grids)	Percentage (%)
Rainfall	Region 1	BCCAQ	1.960204	6137	92.34%
		QDM		6162	92.72%
		ISI-MIP		6515	98.03%
	Region 2	BCCAQ	1.960204	592	90.24%
		QDM		587	89.48%
		ISI-MIP		655	99.85%
	Region 3	BCCAQ	1.960204	3888	70.28%
		QDM		3901	70.52%
		ISI-MIP		5144	92.99%
Temperature Maximum	Region 1	BCCAQ	1.960204	6613	99.50%
		QDM		6612	99.49%
		ISI-MIP		6542	98.44%
	Region 2	BCCAQ	1.960204	650	99.09%
		QDM		654	99.70%
		ISI-MIP		656	100.00%
	Region 3	BCCAQ	1.960204	5530	99.96%
		QDM		5528	99.93%
		ISI-MIP		5526	99.89%

Rainfall has a significant level of 70 - 92%, where the highest percentage is in Region 1. The ISI-MIP method is reliable in all regions compared to other methods. The percentage significance of the maximum temperature variable reaches 98 - 100%. The skills of the three methods have almost the same performance, the ISI-MIP method shows its reliability in Region 2 which reaches a perfect percentage. To clarify the method that has the best ability to present the local climate, we try to represent the three methods in a Taylor diagram. In this study, Taylor diagram for each region will be calculated in historical scenarios, both seasonal and non-seasonal. The season in this study is divided into 4 periods, namely the transition period March April May (MAM) September October November (SON), the rainy period is December January February (DJF), and the dry period is June July August (JJA), the division of the season period in Indonesia being 4 periods with refers to Aldrian and Narulita [1, 44].

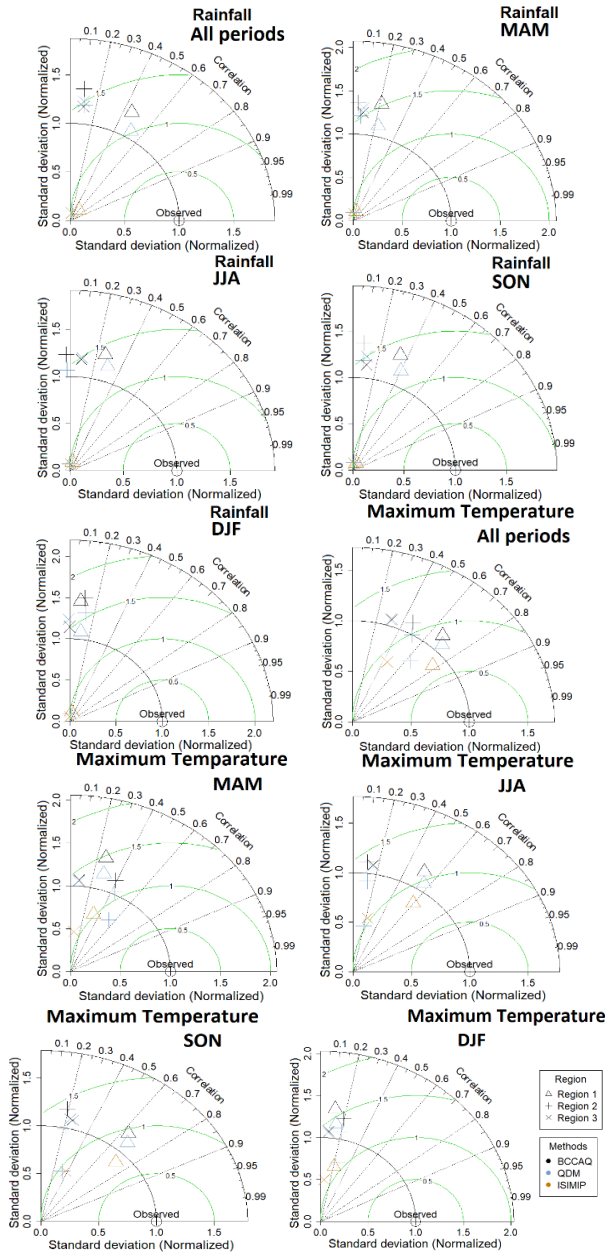

Figure 4: Taylor Diagram.

Based on Figure 4 it can be seen that both rainfall and maximum temperature resulted from the ISI-MIP method consistently have better skills compared to the BCCAQ and QDM methods. The ISI-MIP method has a correlation of around 0.6, greater than the BCCAQ and QDM methods. The SON season is the best season compared to other seasons. The highest correlation in the SON season was found in a previous study by Narulita [48], where SON is a transition from the dry season to the rainy season. In the temperature templates, the maximum correlation of the ISI-MIP method in Region 1 reaches 0.79 and in seasonal SON it reaches 0.71. ESM output in Region 1 can follow the ERA-Interim ECMWF pattern for seasonal and non-seasonal (all periods) compared to Region 2 and Region 3. It can be seen based on the correlation value in each region, where Region 1 has the highest correlation in rainfall variable or maximum temperature.

Projection of Rx1Day and TXx

Expert Team on Climate Change Detection and Indices (ETCCDI) has 27 climate change indices included TXx and Rx1Day. Figure 5 indicates that the rainfall generated by MIROC-ESM of G4 and RCP4.5 scenarios in 2020 - 2100 is highly volatile with a level of about 0.4 - 0.98 mm^2. The G4 scenario can cool the earth, as evidenced by the clear difference between the G4 and RCP4.5 scenarios at the maximum temperature variable. In 2070 the G4 scenario temperature begins to rise and rebound to the level of RCP4.5. To find out how effective the G4 is in reducing the surface temperature of the earth, we calculate the temperature difference between G4 and RCP4.5 during the injection period (2020 - 2069) and post-termination periods (2070 - 2100), as presented in Figure 6.

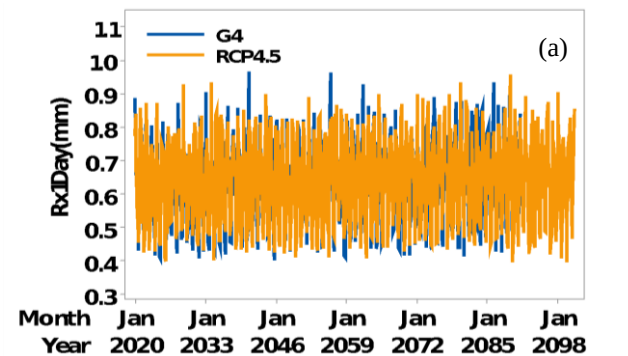

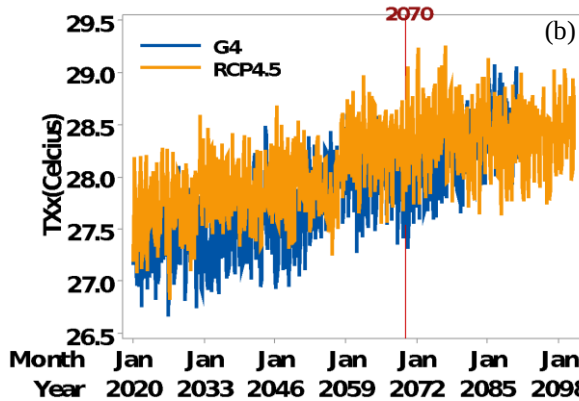

Figure 5: Extreme Index; (a) Rx1Day, and (b) TXx.

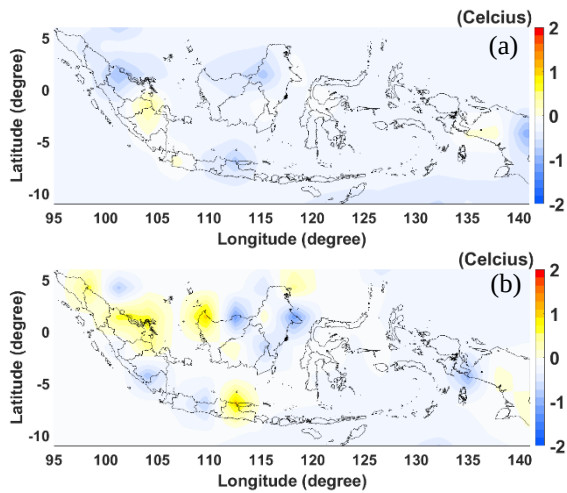

Figure 6: Difference in TXx Index of G4 and RCP4.5 scenarios; (a) period 2020 – 2069, and (b) period 2070 - 2100.

Conclusion

The downscaling and bias correction methods have been proven to be able to resemble the local climate well. The correlation values obtained are significant, where the values for maximum temperature are higher than

rainfall. The percentage of the significant grids for the rainfall variable is more than 70% while the maximum temperature is above 95%. The best method based on Taylor diagram is ISI-MIP. The ISI-MIP method in the transition season SON has a better performance than other seasons. The G4 scenario is proven to be able to reduce the maximum temperature greater than without SRM. The surface temperature of the earth in all regions of Indonesia under SRM will be decreased, but within the post-termination periods, the temperature over East Java, parts of Kalimantan, and Sumatra begin to heat up.

Acknowledgment

Acknowledge the Ministry of Research and Technology (RISTEKBRIN) and the Indonesian Ministry of Education and Culture (KEMENDIKBUD) for their financial support. Partial supports from PEER project as well as DECIMAL project are also acknowlegded.

References

[1] E. Aldrian and R. Dwi Susanto, "Identification of three dominant rainfall regions within Indonesia and their relationship to sea surface temperature," *Int. J. Climatol.*, vol. 23, no. 12, pp. 1435–1452, 2003.

[2] I. G. Hendrawan, K. Asai, A. Triwahyuni, and D. V. Lestari, "The interannual rainfall variability in Indonesia corresponding to El Niño Southern Oscillation and Indian Ocean Dipole," *Acta Oceanol. Sin.*, vol. 38, no. 7, pp. 57–66, 2019.

[3] H. H. Hendon and B. Liebmann, "A Composite Study of Onset of the Australian Summer Monsoon," *Journal of the Atmospheric Sciences*, vol. 47, no. 18. pp. 2227–2240, 2002.

[4] T. R. Anderson, E. Hawkins, and P. D. Jones, "CO_2, the greenhouse effect and global warming: from the pioneering work of Arrhenius and Callendar to today's Earth System Models," *Endeavour*, vol. 40, no. 3, pp. 178–187, 2016.

[5] Intergovernmental Panel on Climate, *Global Warming of 1.5°C an IPCC special report on the impacts of global warming of 1.5 °C above pre-industrial levels and related global greenhouse gas emission pathways, in the context of strengthening the global response to the threat of climate change,*. Switzerland: IPCC, 2018.

[6] N. Jha, "Environment, Sustainability and Mechanical Engineering," 2018.

[7] R. Oktaviani, S. Amaliah, C. Ringler, M. W. Rosegrant, and T. B. Sulser, *The impact of global climate change on the Indonesian economy.*

Washington, D.C.: IFPRI, 2011.
[8] H. Kuswanto, M. Salamah, S. M. Retnaningsih, and D. D. Prastyo, "On the Impact of Climate Change to Agricultural Productivity in East Java," *J. Phys. Conf. Ser.*, vol. 979, no. 1, pp. 0–8, 2018.
[9] I. R. Abubakar and U. L. Dano, "Sustainable urban planning strategies for mitigating climate change in Saudi Arabia," *Environ. Dev. Sustain.*, vol. 22, no. 6, pp. 5129–5152, 2020.
[10] Y. Suryadi, D. N. Sugianto, and Hadiyanto, "Climate Change in Indonesia (Case Study: Medan, Palembang, Semarang)," *E3S Web Conf.*, vol. 31, pp. 3–8, 2018.
[11] S. B. Sipayung *et al.*, "Analysis of Drought Potential in Sumba Island until 2040 Caused by Climate Change," *J. Phys. Conf. Ser.*, vol. 1373, no. 1, pp. 1-12, 2019.
[12] H. Kuswanto, K. Fithriasari, and R. Inas, "Drought risk mapping in East Nusa Tenggara Indonesia based on return periods," *Asian J. Sci. Res.*, vol. 11, no. 4, pp. 489–497, 2018.
[13] B. Kravitz *et al.*, "The Geoengineering Model Intercomparison Project (GeoMIP)," *Atmos. Sci. Lett.*, vol. 12, no. 2, pp. 162–167, 2011.
[14] C. H. Trisos, C. Gabriel, A. Robock, and L. Xia, "Chapter 24 - Ecological, Agricultural, and Health Impacts of Solar Geoengineering," in *Resilience*, Z. Zommers and K. Alverson, Eds. Elsevier, pp. 291–303, 2018.
[15] P. Zhan, W. Zhu, T. Zhang, X. Cui, and N. Li, "Impacts of Sulfate Geoengineering on Rice Yield in China: Results From a Multimodel Ensemble," *Earth's Futur.*, vol. 7, no. 4, pp. 395–410, 2019.
[16] B. Parkes, A. Challinor, and K. Nicklin, "Crop failure rates in a geoengineered climate: Impact of climate change and marine cloud brightening," *Environ. Res. Lett.*, vol. 10, no. 8, 2015.
[17] L. Xia *et al.*, "Solar radiation management impacts on agriculture in China: A case study in the GeoengineeringModel Intercomparison Project (GeoMIP)," *J. Geophys. Res. Atmos.*, vol. 119, pp. 8695–8711, 2014.
[18] M. Zilli *et al.*, "The impact of climate change on Brazil's agriculture," *Sci. Total Environ.*, vol. 740, pp. 139384, 2020.
[19] U. Effiong and R. L. Neitzel, "Assessing the direct occupational and public health impacts of solar radiation management with stratospheric aerosols.," *Environ. Health*, vol. 15, pp. 7, Jan. 2016.
[20] R. Gunderson, D. Stuart, and B. Petersen, "The Political Economy of Geoengineering as Plan B: Technological Rationality, Moral Hazard, and New Technology," *New Polit. Econ.*, vol. 24, no. 5, pp. 696–715, 2019.
[21] K. K. Ott, "On the political economy of Solar Radiation Management," *Front. Environ. Sci.*, vol. 6, no. June, pp. 1–13, 2018.
[22] A. Aaheim *et al.*, "An economic evaluation of solar radiation management," *Sci. Total Environ.*, vol. 532, pp. 61–69, 2015.
[23] D. Ji *et al.*, "Extreme temperature and precipitation response to solar

dimming and stratospheric aerosol geoengineering," *Atmos. Chem. Phys.*, vol. 18, no. 14, pp. 10133–10156, 2018.
[24] B. Kravitz *et al.*, "A multi-model assessment of regional climate disparities caused by solar geoengineering," *Environ. Res. Lett.*, vol. 9, no. 7, 2014.
[25] P. J. Irvine *et al.*, "Towards a comprehensive climate impacts assessment of solar geoengineering," *Earth's Futur.*, vol. 5, no. 1, pp. 93–106, 2017.
[26] I. Pinto, C. Jack, C. Lennard, S. Tilmes, and R. C. Odoulami, "Africa's Climate Response to Solar Radiation Management With Stratospheric Aerosol," *Geophys. Res. Lett.*, vol. 47, no. 2, pp. 1–10, 2020.
[27] K. Karami, S. Tilmes, H. Muri, and S. V. Mousavi, "Storm Track Changes in the Middle East and North Africa Under Stratospheric Aerosol Geoengineering," *Geophys. Res. Lett.*, vol. 47, no. 14, 2020. in West African Summer Monsoon Precipitation Under Stratospheric Aerosol Geoengineering," *Earth's Futur.*, vol. 8, no. 7, 2020.
[29] A. H. Wigena, "Pemodelan Statistical Downscaling Dengan Regresi Projection Pursuit Untuk Peramalan Curah Hujan Bulanan (Kasus Curah hujan bulanan di Indramayu)," *Disertation*, 2006.
[30] E. P. Salathe Jr, P. W. Mote, and M. W. Wiley, "Review of scenario selection and downscaling methods for the assessment of climate change impacts on hydrology in the United States pacific northwest," *Int. J. Climatol.*, vol. 27, no. 12, pp. 1611–1621, 2007.
[31] A. W. Wood, L. R. Leung, V. Sridhar, and D. P. Lettenmaier, "Hydrologic implications of dynamical and statistical approaches to downscaling climate model outputs," *Clim. Change*, vol. 62, no. 1–3, pp. 189–216, 2004.
[32] S. Hagemann, C. Chen, J. O. Haerter, J. Heinke, D. Gerten, and C. Piani, "Impact of a Statistical Bias Correction on the Projected Hydrological Changes Obtained from Three GCMs and Two Hydrology Models," *J. Hydrometeorol.*, vol. 12, pp. 556–578, 2011.
[33] S. Hempel, K. Frieler, L. Warszawski, J. Schewe, and F. Piontek, "A trend-preserving bias correction – the ISI-MIP approach," pp. 219–236, 2013.
[34] A. J. Cannon, S. R. Sobie, and T. Q. Murdock, "Bias correction of GCM precipitation by quantile mapping: How well do methods preserve changes in quantiles and extremes?," *J. Clim.*, vol. 28, no. 17, pp. 6938–6959, 2015.
[35] A. T. Werner and A. J. Cannon, "Hydrologic extremes -- an intercomparison of multiple gridded statistical downscaling methods," *Hydrol. Earth Syst. Sci.*, vol. 20, no. 4, pp. 1483–1508, 2016.
[36] M. A. Sunyer, H. Madsen, and P. H. Ang, "A comparison of different regional climate models and statistical downscaling methods for extreme rainfall estimation under climate change," *Atmos. Res.*, vol. 103, pp. 119–

128, 2012.
[37] M. A. Sarr, O. Seidou, Y. Tramblay, and S. El Adlouni, "Comparison of downscaling methods for mean and extreme precipitation in Senegal," *J. Hydrol. Reg. Stud.*, vol. 4, pp. 369–385, 2015.
[38] M. B. Switanek *et al.*, "Scaled distribution mapping: a bias correction method that preserves raw climate model projected changes," *Hydrol. Earth Syst. Sci.*, vol. 21, no. 6, pp. 2649–2666, 2017.
[39] J. R. Lanzante, D. Adams-Smith, K. W. Dixon, M. Nath, and C. E. Whitlock, "Evaluation of some distributional downscaling methods as applied to daily maximum temperature with emphasis on extremes," *Int. J. Climatol.*, vol. 40, no. 3, pp. 1571–1585, 2020.
[40] J. H. Heo, H. Ahn, J. Y. Shin, T. R. Kjeldsen, and C. Jeong, "Probability distributions for a quantile mapping technique for a bias correction of precipitation data: A case study to precipitation data under climate change," *Water (Switzerland)*, vol. 11, no. 7, 2019.
[41] F. Fauzi, H. Kuswanto, and R. M. Atok, "Bias correction and statistical downscaling of earth system models using quantile delta mapping (QDM) and bias correction constructed analogues with quantile mapping reordering (BCCAQ)," *J. Phys. Conf. Ser.*, vol. 1538, no. 1, 2020.
[42] Y. Kim, C. H. R. Lima, and H. Kwon, "Kriging Approach to Quantile Delta Mapping (QDM) for Spatial Downscaling of Climate Change Scenario," pp. 20829, 2021.
[43] Y. Tong, X. Gao, Z. Han, Y. Xu, Y. Xu, and F. Giorgi, "Bias correction of temperature and precipitation over China for RCM simulations using the QM and QDM methods," *Clim. Dyn.*, no. 0123456789, 2020.
[44] R. H. Moss *et al.*, "The next generation of scenarios for climate change research and assessment," *Nature*, vol. 463, no. 7282, pp. 747–756, 2010.
[45] H. G. Hidalgo, D. M. D., and D. R. Cayan, "Downscaling with constructed analogues: Daily precipitation and temperature fields over the United States," 2008. [Online]. Available: http://tenaya.ucsd.edu/wawona-m/downscaled/supporting_materials/CEC-500-2007-123.pdf.
[46] K. E. Taylor, "Summarizing multiple aspects of model performance in a single diagram," *J. Geophys. Res.*, vol. 106, no. D7, pp. 7183–7192, 2001.
[47] M. G. Donat *et al.*, "Updated analyses of temperature and precipitation extreme indices since the beginning of the twentieth century: The HadEX2 dataset," *J. Geophys. Res. Atmos.*, vol. 118, no. 5, pp. 2098–2118, 2013.
[48] I. Narulita, "Pengaruh ENSO dan IOD pada Variabilitas Curah Hujan diDAS Cerucuk, pulau Belitung," *J. Tanah dan Iklim*, vol. 41, no. 1, pp. 45, 2020.